

Article

# A Demonstration of Pt L<sub>3</sub>-Edge EXAFS Free from Au L<sub>3</sub>-Edge Using Log–Spiral Bent Crystal Laue Analyzers

Yuki Wakisaka <sup>1,\*</sup>, Daiki Kido <sup>1</sup>, Hiromitsu Uehara <sup>1</sup>, Qiuyi Yuan <sup>1</sup>, Satoru Takakusagi <sup>1</sup>, Yohei Uemura <sup>2</sup>, Toshihiko Yokoyama <sup>2</sup>, Takahiro Wada <sup>3</sup> , Motohiro Uo <sup>3</sup>, Tomohiro Sakata <sup>4</sup>, Oki Sekizawa <sup>4,5</sup>, Tomoya Uruga <sup>4,5</sup>, Yasuhiro Iwasawa <sup>4</sup> and Kiyotaka Asakura <sup>1,\*</sup> 

<sup>1</sup> Institute for Catalysis, Hokkaido University, Hokkaido 001-0021, Japan; d-kido@eis.hokudai.ac.jp (D.K.); uehara@oeic.hokudai.ac.jp (H.U.); qy.qiuyiyuan@gmail.com (Q.Y.); takakusa@cat.hokudai.ac.jp (S.T.)

<sup>2</sup> Institute for Molecular Science, Aichi 444-8585, Japan; y-uemura@ims.ac.jp (Y.U.); yokoyama@ims.ac.jp (T.Y.)  
<sup>3</sup> Graduate School of Medical and Dental Sciences, Tokyo Medical and Dental University, Tokyo 113-8549, Japan; wada.abm@tmd.ac.jp (T.W.); uo.abm@tmd.ac.jp (M.U.)

<sup>4</sup> Innovation Research Center for Fuel Cells, The University of Electro-Communications, Tokyo 182-8585, Japan; s-tomohiro@uec.ac.jp (T.S.); sekizawa@uec.ac.jp (O.S.); urugat@spring8.or.jp (T.U.); iwasawa@pc.uec.ac.jp (Y.I.)

<sup>5</sup> Japan Synchrotron Radiation Research (JASRI), Hyogo 679-5148, Japan

\* Correspondence: ywkskhkd@gmail.com (Y.W.); askr@cat.hokudai.ac.jp (K.A.); Tel.: +81-11-706-9113(K.A.)

Received: 30 March 2018; Accepted: 8 May 2018; Published: 13 May 2018



**Abstract:** Pt-Au nanostructures are important and well-studied fuel cell catalysts for their promising catalytic performance. However, a detailed quantitative local structure analysis, using extended X-ray absorption fine structure (EXAFS) spectroscopy, have been inhibited by interference between Pt and Au L<sub>3</sub>-edges. In this paper, Pt L<sub>3</sub>-edge XAFS analysis, free of Au L<sub>3</sub> edge, is demonstrated for a Pt-Au reference sample using a low-cost log–spiral bent crystal Laue analyzer (BCLA). This method facilitates the EXAFS structural analysis of Pt-Au catalysts, which are important to improve fuel cell catalysts.

**Keywords:** Pt-Au; XAFS; BCLA

## 1. Introduction

Platinum is one of the key elements for catalytic reactions in fuel cells. Although there are many studies in which authors suggest different methodologies to replace Pt with others low-cost metals, it is still difficult to substitute the catalytic performance of Pt. A practical approach, combining different metals with Pt have widely been adopted to reduce the amount of Pt and improve its activity and durability. Among those, Au is one of the interesting metals due to its superior oxygen-reduction-reaction activity and durability reported in Pt-Au nanostructures, where the Pt (shell)-Au (core) structures and the effect of Au decoration on the edges of Pt surfaces are used as a fuel cell catalyst [1–5]. Hence, it is essential to understand the local structures of both Pt and Au in an atomic scale to elucidate the mechanism of the catalytic reactions in Pt-Au nanostructures. Extended X-ray absorption fine structure (extended XAFS or EXAFS) spectroscopy is a suitable and widely-used method to investigate the local atomic structures of fuel-cell catalysts because of its atomic selectivity and applicability to nanoparticles under electrochemical environments [6]. However, in case of Pt-Au system, it is difficult to obtain a Pt L<sub>3</sub>-edge EXAFS sufficient for its analysis due to the interference between Pt and Au, which are only separated by ~350 eV, so that Au L<sub>3</sub>-edge appears at ~9.6 Å<sup>-1</sup> in Pt L<sub>3</sub>-edge EXAFS [7,8]. Although the problem can be solved by measuring K-edge XAFS, where Pt and Au K-edges are separated by

~2300 eV [9,10], the information in the long-range order is limited by the lifetime broadening, and Pt  $L_3$ -edge EXAFS measurement is preferable.

Glatzel et al. first demonstrated that EXAFS spectra sufficient for analysis under the existence of interfering absorption edges, called range-extended EXAFS, could be obtained by taking advantage of high-energy-resolution fluorescence detected XAFS (HERFD-XAFS) using crystal analyzers with an energy resolution of ~1 eV [11,12]. It was shown that HERFD-XAFS was not only useful for capturing the detailed structures of the X-ray absorption near edge structure spectra but also capable of obtaining the range extended EXAFS. Recently, this method was applied to the feasibility study of Pt  $L_3$ -edge EXAFS in the presence of Au [13]. In this paper, we demonstrated that range-extended Pt  $L_3$ -edge EXAFS can also be obtained under the existence of Au using a log-spiral bent crystal Laue analyzer (BCLA) [14]. Although the energy resolution of BCLA (>10 eV [15]) is generally less than the resolution of crystal analyzers used in HERFD-XAFS (~1 eV), the energy resolution of the BCLA is sufficiently small for discriminating Au fluorescence from Pt. On the other hand, adopting BCLA, one can expect a lower cost for experimental arrangement compared to HERFD-XAFS. Moreover, the emission energy scan of BCLA can be achieved by a vertical scan because it approximately corresponds to the change in the incident angle of the X-ray against the crystal face. These characteristics may facilitate the application of the BCLA to the range-extended EXAFS of Pt-Au catalysts.

## 2. Results

Figure 1 shows the emission X-ray intensity from a diluted Pt-Au reference sample measured through a BCLA moved to the vertical direction. The incident X-ray energy was 12.1 keV, which was corresponding to the energy above the Au  $L_3$ -edge. All four fluorescent peaks (Pt  $L_{\alpha 2}$ , Pt  $L_{\alpha 1}$ , Au  $L_{\alpha 2}$ , Au  $L_{\alpha 1}$ ) were well resolved, and it is confirmed that there was a clear correspondence between the accepted X-ray fluorescent energy and the vertical position of the BCLA. Au fluorescent peaks were smaller compared to the expected molar ratio of the sample (Pt/Au = ~1/10); a solid-state detector (SSD) was used within the range of interest, only including the entire Pt  $L_{\alpha}$  peaks. According to the full width half maximum (FWHM) of the Pt  $L_{\alpha 1}$  peak, the energy resolution is ~30 eV for this experimental arrangement.

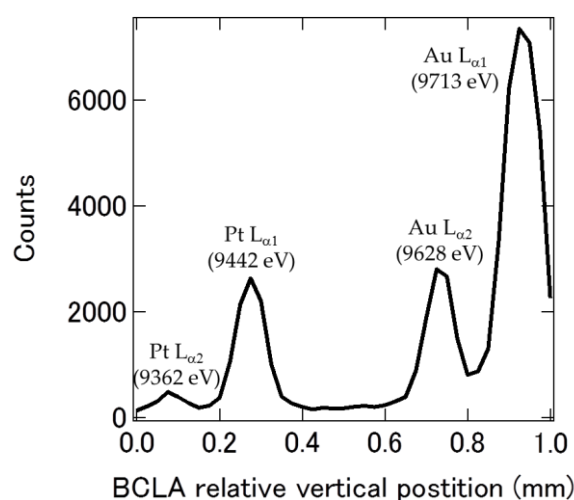


**Figure 1.** Emission X-ray intensity from a diluted Pt-Au sample measured through a BCLA moved to the vertical direction. Four peaks were assigned as Pt  $L_{\alpha 2}$ , Pt  $L_{\alpha 1}$ , Au  $L_{\alpha 2}$ , Au  $L_{\alpha 1}$ , from lower to higher positions of the BCLA.

Figure 2 shows the normalized XAFS spectra of a concentrated Pt-Au reference sample measured in a transmission mode and a fluorescence mode with the BCLA. The edge heights of the raw spectrum were 1 and 7.31.1 for Pt and Au, respectively. It was clearly observed by the transmission spectrum

that the sample contained ~10 times more Au than Pt. In the fluorescence mode, apparently, no Au signal was observed due to the BCLA. However, the Pt fluorescence signal abruptly decreased at the Au L<sub>3</sub>-edge; the incident X-rays were absorbed by the abundant Au atoms. Consequently, Pt atoms were less excited [11,16]. This effect can be avoided by a sufficient dilution of the sample.

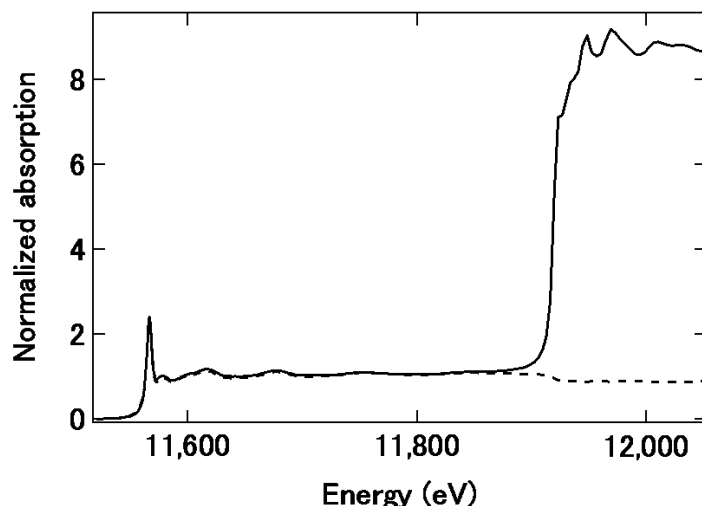


**Figure 2.** XAFS spectra of the concentrated Pt-Au reference sample measured in transmission (solid line) and fluorescence mode (dashed line) with the BCLA. The spectrum was normalized by the edge height of Pt = 1.

Figure 3a shows the XAFS spectrum of the diluted Pt-Au reference sample (see Materials and Methods) measured in the fluorescence mode with the BCLA. The edge heights of the raw data for this diluted sample measured in transmission mode was 0.007 for Pt and 0.05 for Au, respectively. As expected, no clear anomaly was observed near the region of Au L<sub>3</sub>-edge, when the interference of Au and Pt L<sub>3</sub>-edge EXAFS could be removed. Figure 3b shows the  $k^3\chi$  plot with an accumulation time of less than 30 min. For comparison, the Pt L<sub>3</sub> transmission XAFS spectrum of a standard sample (PtCl<sub>4</sub>) measured at Beam line (BL)14B2 in Super Photon ring-8 GeV (SPring-8) was overlaid as a red dashed line (see Figure 3b). There is a good agreement up to  $\sim 12 \text{ \AA}^{-1}$ . No clear edge was found even in this  $k^3\chi$  plot. Here, we demonstrated that Pt L<sub>3</sub>-edge EXAFS spectra, free of Au L<sub>3</sub>-edge, could be obtained using a considerable amount of Au in BCLA.

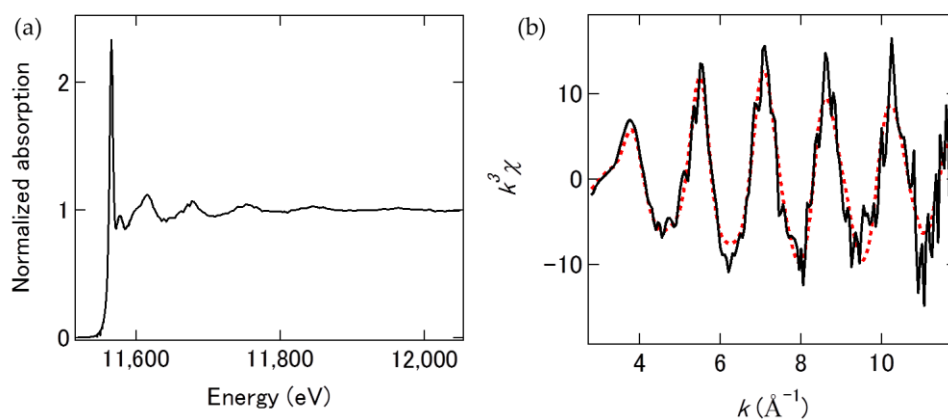


**Figure 3.** (a): Fluorescence XAFS spectrum of the diluted Pt-Au reference sample measured with the BCLA. The spectrum was normalized by the edge height of Pt = 1; (b):  $k^3\chi$  EXAFS spectra of the diluted Pt-Au reference sample measured at BL36XU (black solid line) and of the standard sample PtCl<sub>4</sub> (red dashed line) measured at BL14B2.

### 3. Discussion

Previously, range-extended EXAFS was only achieved in HERFD-XAFS. In this work, we have successfully demonstrated the range-extended EXAFS analysis using BCLA is possible. BCLA has several advantages mentioned above compared to HERFD-XAFS method. In addition, the crystal alignment is quite simple. It is mainly achieved by a vertical scan followed by a precise two-dimensional linear scan of the BCLA [15,17]. The only constraint is the vertical size of the incident X-ray beam. In this study, it was  $\sim 50 \mu\text{m}$ , though this condition is not fixed, depending on the energy difference between the measuring (Pt) and interfering (Au) fluorescent X-rays (see Figure 1).

HERFD-XAFS is, in general, a powerful technique to detect the subtle spectral changes in X-ray absorption near to edge regions. By applying this technique to Pt catalysts in fuel cells, various adsorbates on Pt and its oxidation states have been discussed [18–20]. HERFD-XAFS can not be achieved by using the BCLA because of their moderate energy resolution larger than the core-hole lifetime broadening. However, this is preferable in case of direct comparison between the spectra measured in the transmission and the fluorescence mode using BCLA; which should have the same energy resolutions.

### 4. Materials and Methods

The concentrated Pt-Au reference sample was made by mixing  $\text{PtCl}_4$  and AuCl powder. The mixture was then ground in a mortar and pestle together with BN (boron nitride) powder and pressed into a pellet with a size of 1 mm thick and 10 mm diameter. The Pt and Au concentration was Pt/Au  $\sim 1/10$  and the Pt  $L_3$ -edge step ( $\Delta\mu t$ ) was  $\sim 0.1$ . The diluted Pt-Au reference sample was made diluting the concentrated Pt-Au pellet by  $\sim 1/20$  with additional BN powder.

The XAFS measurements were performed at BL36XU in SPring-8 (JASRI, Koto, Japan). The beam size of the incident X-rays was focused to  $\sim 50 \mu\text{m}$  (vertical)  $\times \sim 500 \mu\text{m}$  (horizontal) by using 4 focusing mirrors equipped in the beamline. The photon flux was  $\sim 2 \times 10^{13}$  photons/s, but it was reduced to  $\sim 2 \times 10^{12}$  photons/s for the diluted Pt-Au sample using an Al attenuator. Ion chambers were used for the transmission measurement. A commercial BCLA (0095, FMB Oxford, UK) and a 25-element Ge SSD (Canberra, Conneticut, USA) or a pixel-array detector (PILATUS 300K-W; Dectris, Baden-Daettwil, Switzerland) were used for detecting fluorescent X-rays. The sample and the BCLA/SSD (or PILATUS) were placed in the  $45^\circ/45^\circ$  arrangement. The shaping time of the SSD was set to 0.5  $\mu\text{s}$ , which resulted in an SSD energy resolution of 400 eV. The region of interest in the SSD was 9.09–9.76 keV. Thus, the Au fluorescence effect cannot fully suppress after the Au  $L_3$ -edge. The commercial BCLA was linearly scanned in two dimensions to find their optimum position so that the Pt  $L_{\alpha 1}$  fluorescent X-ray intensity became maximum in the multi-element SSD. Only the detector of elements in the multi-element SSD, which sufficiently suppressed Au  $L_{\alpha}$  fluorescent X-rays, was used for the spectral analyses [21].

### 5. Conclusions

Pt  $L_3$ -edge XAFS analysis, free from Au  $L_3$ -edge, was demonstrated here for the first time using BCLA; a low-cost and high-sensitive crystal analyzers, which facilitates detail EXAFS analyses for Pt-Au fuel cell catalysts. Our results confirm the feasibility of the range-extended EXAFS using BCLA, we apply this technique to two interesting fuel cell models containing Pt and Au; Au-Pt-Co-N nanoparticles deposited on a highly oriented pyrolytic graphite [22] and monolayer Pt deposited on Au thin film with 60 nm thickness on a Si (100) substrate [23]. We will soon report these results.

**Author Contributions:** Y.W., H.U., and K.A. conceived, designed, and performed the experiments; D.K., Q.Y., Y.U., and T.W. performed the experiments; Y.W., S.T., M.U., T.Y., T.U., Y.I., and K.A. discussed the results; T.S., O.S., and T.U. supported the experiments; Y.W. analyzed the data; Y.W. and K.A. wrote the paper.

**Acknowledgments:** The authors would like to express their gratitude to the New Energy and Industrial Technology Development Organization (NEDO) Polymer Electrolyte Fuel Cell project for their financial support. We would like to thank Hiroyuki Asakura for discussing the range-extended EXAFS results of Pt-Au. T.W. and Y.U. were supported by the Cooperative Research Program of Institute for Catalysis, Hokkaido University. The XAFS

measurements at SPring-8 were performed under project number 2016A7902 and 2016B7902. XAFS spectrum of standard sample PtCl<sub>4</sub> is utilized by SPring-8 BL14B2 XAFS database (2014S0000-000523). This work was supported by the Technical Division of Institute for Catalysis, Hokkaido University.

**Conflicts of Interest:** The authors declare no conflict of interest.

## References

1. Kristian, N.; Wang, X. Pt shell–Au core/C electrocatalyst with a controlled shell thickness and improved Pt utilization for fuel cell reactions. *Electrochem. Commun.* **2008**, *10*, 12–15. [[CrossRef](#)]
2. Shuangyin, W.; Noel, K.; Sanping, J.; Xin, W. Controlled synthesis of dendritic Au@Pt core–shell nanomaterials for use as an effective fuel cell electrocatalyst. *Nanotechnology* **2009**, *20*, 025605. [[CrossRef](#)]
3. Xiu, C.; Shengnan, W.; Scott, J.; Zhibing, C.; Zhenghua, W.; Lun, W.; Li, Y. The deposition of Au–Pt core-shell nanoparticles on reduced graphene oxide and their catalytic activity. *Nanotechnology* **2013**, *24*, 295402. [[CrossRef](#)]
4. Dai, Y.; Chen, S. Oxygen Reduction Electrocatalyst of Pt on Au Nanoparticles through Spontaneous Deposition. *ACS Appl. Mater. Interfaces* **2015**, *7*, 823–829. [[CrossRef](#)] [[PubMed](#)]
5. Takahashi, S.; Chiba, H.; Kato, T.; Endo, S.; Hayashi, T.; Todoroki, N.; Wadayama, T. Oxygen reduction reaction activity and structural stability of Pt–Au nanoparticles prepared by arc-plasma deposition. *Phys. Chem. Chem. Phys.* **2015**, *17*, 18638–18644. [[CrossRef](#)] [[PubMed](#)]
6. Iwasawa, Y.; Asakura, K.; Tada, M. *XAFS Techniques for Catalysts, Nanomaterials, and Surfaces*; Springer: New York, NY, USA, 2016.
7. Nagamatsu, S.; Arai, T.; Yamamoto, M.; Ohkura, T.; Oyanagi, H.; Ishizaka, T.; Kawanami, H.; Uruga, T.; Tada, M.; Iwasawa, Y. Potential-Dependent Restructuring and Hysteresis in the Structural and Electronic Transformations of Pt/C, Au(Core)–Pt(Shell)/C, and Pd(Core)–Pt(Shell)/C Cathode Catalysts in Polymer Electrolyte Fuel Cells Characterized by in Situ X-ray Absorption Fine Structure. *J. Phys. Chem. C* **2013**, *117*, 13094–13107.
8. Yuan, Q.; Takakusagi, S.; Wakisaka, Y.; Uemura, Y.; Wada, T.; Ariga, H.; Asakura, K. Polarization-dependent Total Reflection Fluorescence X-ray Absorption Fine Structure (PTRF–XAFS) Studies on the Structure of a Pt Monolayer on Au(111) Prepared by the Surface-limited Redox Replacement Reaction. *Chem. Lett.* **2017**, *46*, 1250–1253. [[CrossRef](#)]
9. Kaito, T.; Mitsumoto, H.; Sugawara, S.; Shinohara, K.; Uehara, H.; Ariga, H.; Takakusagi, S.; Hatakeyama, Y.; Nishikawa, K.; Asakura, K. K-Edge X-ray Absorption Fine Structure Analysis of Pt/Au Core–Shell Electrocatalyst: Evidence for Short Pt–Pt Distance. *J. Phys. Chem. C* **2014**, *118*, 8481–8490. [[CrossRef](#)]
10. Kaito, T.; Mitsumoto, H.; Sugawara, S.; Shinohara, K.; Uehara, H.; Ariga, H.; Takakusagi, S.; Asakura, K. A new spectroelectrochemical cell for in situ measurement of Pt and Au K-edge X-ray absorption fine structure. *Rev. Sci. Instrum.* **2014**, *85*, 084104. [[CrossRef](#)] [[PubMed](#)]
11. Glatzel, P.; de Groot, F.M.F.; Manoilova, O.; Grandjean, D.; Weckhuysen, B.M.; Bergmann, U.; Barrea, R. Range-extended EXAFS at the L<sub>2,3</sub> edge of rare earths using high-energy-resolution fluorescence detection: A study of La in LaOCl. *Phys. Rev. B* **2005**, *72*, 014117. [[CrossRef](#)]
12. Yano, J.; Pushkar, Y.; Glatzel, P.; Lewis, A.; Sauer, K.; Messinger, J.; Bergmann, U.; Yachandra, V. High-Resolution Mn EXAFS of the Oxygen-Evolving Complex in Photosystem II: Structural Implications for the Mn<sub>4</sub>Ca Cluster. *J. Am. Chem. Soc.* **2005**, *127*, 14974–14975. [[CrossRef](#)] [[PubMed](#)]
13. Asakura, H.; Kawamura, N.; Mizumaki, M.; Nitta, K.; Ishii, K.; Hosokawa, S.; Teramura, K.; Tanaka, T. A feasibility study of “range-extended” EXAFS measurement at the Pt L<sub>3</sub>-edge of Pt/Al<sub>2</sub>O<sub>3</sub> in the presence of Au<sub>2</sub>O<sub>3</sub>. *J. Anal. At. Spectrom.* **2018**, *33*, 84–89. [[CrossRef](#)]
14. Zhong, Z.; Chapman, L.D.; Bunker, B.A.; Bunker, G.B.; Fischetti, R.; Segre, C.U. A bent Laue analyzer for fluorescence EXAFS detection. *J. Synchrotron Radiat.* **1999**, *6*, 212–214. [[CrossRef](#)] [[PubMed](#)]
15. Kujala, N.G.; Karanfil, C.; Barrea, R.A. High resolution short focal distance Bent Crystal Laue Analyzer for copper K edge X-ray absorption spectroscopy. *Rev. Sci. Instrum.* **2011**, *82*, 063106. [[CrossRef](#)] [[PubMed](#)]
16. Bianchini, M.; Glatzel, P. A tool to plan photon-in/ photon-out experiments: Count rates, dips and self-absorption. *J. Synchrotron Radiat.* **2012**, *19*, 911–919. [[CrossRef](#)] [[PubMed](#)]
17. Karanfil, C.; Bunker, G.; Newville, M.; Segre, C.U.; Chapman, D. Quantitative performance measurements of bent crystal Laue analyzers for X-ray fluorescence spectroscopy. *J. Synchrotron Radiat.* **2012**, *19*, 375–380. [[CrossRef](#)] [[PubMed](#)]

18. Friebel, D.; Viswanathan, V.; Miller, D.J.; Anniyev, T.; Ogasawara, H.; Larsen, A.H.; O'Grady, C.P.; Nørskov, J.K.; Nilsson, A. Balance of Nanostructure and Bimetallic Interactions in Pt Model Fuel Cell Catalysts: In Situ XAS and DFT Study. *J. Am. Chem. Soc.* **2012**, *134*, 9664–9671. [[CrossRef](#)] [[PubMed](#)]
19. Merte, L.R.; Behafarid, F.; Miller, D.J.; Friebel, D.; Cho, S.; Mbuga, F.; Sokaras, D.; Alonso-Mori, D.; Weng, T.-C.; Nordlund, D.; et al. Electrochemical Oxidation of Size-Selected Pt Nanoparticles Studied Using in Situ High-Energy-Resolution X-ray Absorption Spectroscopy. *ACS Catal.* **2012**, *2*, 2371–2376. [[CrossRef](#)]
20. Cui, Y.-T.; Harada, Y.; Niwa, H.; Hatanaka, T.; Nakamura, N.; Ando, M.; Yoshida, T.; Ishii, K.; Matsumura, D.; Oji, H.; et al. Wetting Induced Oxidation of Pt-based Nano Catalysts Revealed by In Situ High Energy Resolution X-ray Absorption Spectroscopy. *Sci. Rep.* **2017**, *7*, 1482. [[CrossRef](#)] [[PubMed](#)]
21. Wakisaka, Y.; Iwasaki, Y.; Uehara, H.; Mukai, S.; Kido, D.; Takakusgi, S.; Uemura, Y.; Wada, T.; Yuan, Q.; Sekizawa, O.; et al. Approach to Highly Sensitive XAFS by Means of Bent Crystal Laue Analyzers. *J. Surf. Sci. Soc. Jpn.* **2017**, *38*, 378–383. [[CrossRef](#)]
22. Takahashi, S.; Takahashi, N.; Todoroki, N.; Wadayama, T. Dealloying of Nitrogen-Introduced Pt–Co Alloy Nanoparticles: Preferential Core–Shell Formation with Enhanced Activity for Oxygen Reduction Reaction. *ACS Omega* **2016**, *1*, 1247–1252. [[CrossRef](#)]
23. Liu, Y.; Hangarter, C.M.; Garcia, D.; Moffat, T.P. Self-terminating electrodeposition of ultrathin Pt films on Ni: An active, low-cost electrode for H<sub>2</sub> production. *Surf. Sci.* **2015**, *631*, 141–154. [[CrossRef](#)]



© 2018 by the authors. Licensee MDPI, Basel, Switzerland. This article is an open access article distributed under the terms and conditions of the Creative Commons Attribution (CC BY) license (<http://creativecommons.org/licenses/by/4.0/>).